marine ecology

Marine Ecology. ISSN 0173-9565

ORIGINAL ARTICLE

Finding the hotspots within a biodiversity hotspot: fine-scale biological predictions within a submarine canyon using high-resolution acoustic mapping techniques

Katleen Robert[1], Daniel O.B. Jones[2], Paul A. Tyler[1], David Van Rooij[3] & Veerle A.I. Huvenne[2]

1 Ocean and Earth Science, University of Southampton, Southampton, UK
2 National Oceanography Centre, University of Southampton, Southampton, UK
3 Department of Geology and Soil Science, Ghent University, Gent, Belgium

Keywords
Biodiversity; deep-sea ecology; megafauna; predictive habitat modelling; submarine canyons.

Correspondence
Katleen Robert, Ocean and Earth Science, University of Southampton, Waterfront Campus, European Way, Southampton SO14 3ZH, UK.
E-mail: kr2e11@soton.ac.uk

Accepted: 1 September 2014

doi: 10.1111/maec.12228

Abstract

Submarine canyons are complex geomorphological features that have been suggested as potential hotspots for biodiversity. However, few canyons have been mapped and studied at high resolution (tens of m). In this study, the four main branches of Whittard Canyon, Northeast Atlantic, were mapped using multibeam and sidescan sonars to examine which environmental variables were most useful in predicting regions of higher biodiversity. The acoustic maps obtained were ground truthed by 13 remotely operated vehicle (ROV) video transects at depths ranging from 650 to 4000 m. Over 100 h of video were collected, and used to identify and georeference megabenthic invertebrate species present within specific areas of the canyon. Both general additive models (GAMs) and random forest (RF) were used to build predictive maps for megafaunal abundance, species richness and biodiversity. Vertical walls had the highest diversity of organisms, particularly when colonized by cold-water corals such as *Lophelia pertusa* and *Solenosmilia variabilis*. GAMs and RF gave different predictive maps and external assessment of predictions indicated that the most adequate technique varied based on the response variable considered. By using ensemble mapping approaches, results from more than one model were combined to identify vertical walls most likely to harbour a high biodiversity of organisms or cold-water corals. Such vertical structures were estimated to represent less than 0.1% of the canyon's surface. The approach developed provides a cost-effective strategy to facilitate the location of rare biological communities of conservation importance and guide further sampling efforts to help ensure that appropriate monitoring can be implemented.

Introduction

By comparison with other regions of the continental slope, submarine canyons have been proposed as hotspots for biodiversity. Incising the continental shelf, they are typically characterized by high spatial heterogeneity and complex hydrographic patterns, and can act as conduits for larvae and organic matter from the shelf to the deep sea (Vetter & Dayton 1999; Tyler *et al.* 2009; Vetter *et al.* 2010). In addition to increasing habitat heterogeneity at the regional scale (De Leo *et al.* 2010), submarine canyons also exhibit high habitat heterogeneity at the local scale (Huvenne *et al.* 2011), which can result in further finer scale variations in biodiversity. Near-vertical walls within submarine canyons of the Bay of Biscay with particularly high percentage cover of biological growth (particularly cold-water corals, *Lophelia pertusa*, limid bivalves, *Acesta excavata*, and deep-water oysters,

Neopycnodonte zibrowii) have been observed (Van Rooij *et al.* 2010a; Huvenne *et al.* 2011; Johnson *et al.* 2013). Although rare and spatially limited, these structures may provide critical functions as refugia for certain species against anthropogenic impacts such as trawling (Huvenne *et al.* 2011). As fisheries are often associated with the heads of submarine canyons (Morell 2007; Puig *et al.* 2012), it is important to investigate which environmental factors within submarine canyons are responsible for local increases and decreases in biodiversity so that appropriate management and monitoring can be implemented.

Establishing biological spatial patterns is a crucial step in informing conservation measures. However, this is particularly problematic in the deep sea where biological samples are sparse and spatially limited. When investigating broad-scale submarine features characterized by high spatial heterogeneity, only small sections of sea floor may actually harbour high biodiversity or specific species of interest. Without prior knowledge of their likely distributions at high resolutions, important areas may be missed. As full coverage biological sampling is usually not feasible, techniques for producing full coverage predictive maps are being developed. These techniques are based on finding relationships between biological patterns and environmental descriptors derived from high-resolution acoustic maps (Brown *et al.* 2011). Environmental descriptors such as slope, rugosity, aspect (orientation of steepest slope), bathymetric position index (BPI, measure of the relative height of a pixel in comparison to surrounding pixels) and curvature can be derived from bathymetric maps (Wilson *et al.* 2007), whereas sidescan sonar or multibeam backscatter can be used as a proxy for sediment hardness (Lo Iacono *et al.* 2008; Micallef *et al.* 2012). Additional descriptors from sidescan sonar backscatter, such as image texture indices (*e.g.* homogeneity and entropy), skewness or kurtosis, can also be derived to help identify sea-bed composition (Huvenne *et al.* 2007; Blondel & Gómez Sichi 2009; Isachenko *et al.* 2014). Indices specific to canyon morphology, used to compare cross-section profiles, have also been successfully applied (De Leo *et al.* 2014). As acoustic maps can cover larger extents of sea bed much faster than traditional biological sampling techniques (*e.g.* photographs or grabs), predictive maps covering entire regions can be achieved although only limited biological information may be available (McArthur *et al.* 2010). These predictions can act as proxies for biological information until further sampling is possible.

Cold-water corals are one of the vulnerable marine ecosystems of interest as biogenic reefs can maintain particularly high biodiversity both across the reef itself as well as in comparison to the surrounding sea floor (Freiwald *et al.* 2004; Costello *et al.* 2005; Buhl-Mortensen *et al.* 2010; Henry *et al.* 2010). Submarine canyons have been proposed as potentially suitable habitats for cold-water corals as their heterogeneous sea bed provides exposed hard substratum for attachment and canyon morphology creates more complex hydrographic patterns, which may be beneficial for filter-feeders (Mortensen & Buhl-Mortensen 2005; White *et al.* 2005; Orejas *et al.* 2009; Edinger *et al.* 2011). Cold-water corals are also particularly vulnerable to trawling (Fosså *et al.* 2002; Hall-Spencer *et al.* 2002; Roberts *et al.* 2008) and as such, much interest exists for mapping their distributions. Global (Tittensor *et al.* 2009; Davies & Guinotte 2011) and large-scale studies of the Northeast Atlantic (Ross & Howell 2012) have been successful in creating habitat suitability maps, but higher resolution predictive maps are still needed to target specific areas where cold-water corals are likely to occur.

Many studies have found acoustically derived environmental descriptors to be useful in explaining biological distribution patterns and predicting habitat suitability (Dolan *et al.* 2008; Buhl-Mortensen *et al.* 2009; Monk *et al.* 2010). However, few deep-sea studies have employed fine-scale species–environment relationships to build full coverage predictive maps over the full extent of a submarine canyon. In this study, we used environmental descriptors derived from multibeam bathymetry and sidescan sonar backscatter to build full coverage predictive maps for biological characteristics of epibenthic megafauna (including abundance, species richness, biodiversity and cold-water coral presence) across four branches of the Whittard Canyon, Northeast Atlantic. Both general additive models (GAMs) and random forest (RF) were used, and in addition to a split-sample assessment, model predictions are further tested using an externally acquired data set. We also created ensemble maps of the results obtained to identify likely areas for which future sampling might be valuable, particularly with respect to vertical structures.

Material and Methods

Acoustic surveys

During the 2009 RRS *James Cook* 035 cruise, both multibeam (6130 km^2, 50 × 50 m resolution) and sidescan sonar (3800 km^2, 3 × 3 m resolution) surveys were conducted to map the Whittard Canyon, Northeast Atlantic. This submarine canyon is located east of the Goban Spur and links the continental margin of the Celtic Sea (200 m) to the Celtic Fan and Porcupine Abyssal Plain (4000 m) (Fig. 1). Whittard Canyon is a dendritic system composed of four main branches joining at around 3500 m water depth to form a single wider channel.

During the last glacial period, it was part of the drainage system of a palaeovalley (Bourillet *et al.* 2003; Toucanne *et al.* 2008), but its activity is now much reduced owing to its distance from the present-day shoreline (Reid & Hamilton 1990).

The acoustic surveys were conducted using a shipboard EM120 multibeam system and a towed ocean bottom instrument (TOBI) mounted with a 30 kHz sidescan sonar. The bathymetry, processed using the CARIS HIPS & SIPS software suite to a 50-m-resolution grid, (WGS1984, UTM Zone 29N) was used to derive additional environmental layers (50 m resolution) such as slope, SD of slope, aspect (orientation of steepest slope split into two continuous measures: eastness and northness) and curvature (general, plan and profile), based on 3 × 3 pixel size windows. Surface area ratio and bathymetric position index (BPI, using neighbourhood sizes of 150 and 500 m, 1 and 2 km) were also computed (Fig. 2). Flow direction and length layers (downstream to an outlet or sink and upstream from the highest upslope basin point) were also derived as calculating the direction and distance along the flow path of a watershed may provide a proxy for transport within the canyon. Layers were generated in ARCMAP 10 using the 'Spatial Analyst Extension' as well as the 'Land Facet Corridor Tools' and the 'DEM Surface Tools' developed by Jenness Enterprises (Jenness 2012a,b). The TOBI sidescan sonar data were originally processed to a 3 × 3 m resolution grid using the in-house PRISM software suite (Le Bas & Hühnerbach 1998). A 'true slant range' correction (whereby the bathymetry is used instead of an assumed flat sea bed; Le Bas & Huvenne 2009) and an across-track equalization of illumination on an equal range basis were applied during processing and values were normalized to a pixel value of 1000. The higher resolution layer was aggregated to 50 m resolutions by using the mean value in order to conform to the multibeam derived layers. Sidescan sonar backscatter was added to provide information on sea-bed type; high backscatter values are indicative of harder substratum types whereas lower values result from soft sediment absorbing the acoustic signal.

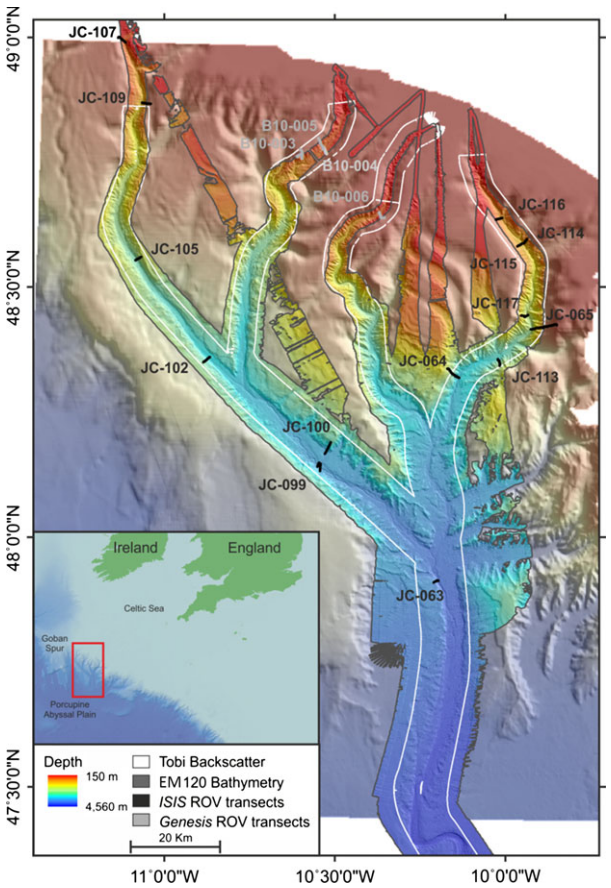

Fig. 1. Map of Whittard Canyon and surveys carried out during the *JC*-010, -035 and -036, and *Belgica* 10/17b cruises. Background bathymetry (201 m resolution) provided by the Geological Survey of Ireland (Dublin).

Benthic imagery

To complement the acoustic maps, 10 video transects were conducted during the *JC*-036 cruise using the workclass *ISIS* remotely operated vehicle (ROV). An additional three transects (dives *JC*-063, -064 and -065) previously collected in 2007 during the *JC*-010 cruise were also added to the benthic imagery data set. These transects were divided across the western and eastern branches of the canyon at depths ranging from 650 to 4000 m (Table 1). With the ROV moving at an average speed of ~0.08 m · s^{-1} and an average height of 3 m off the sea floor, the down-looking colour video camera (Pegasus, Insite Tritech Inc. with SeaArc2 400 W, Deepsea Power&-Light illumination) was recorded on digital tapes and later converted to .mov using a Sony digital HD videocassette recorder. In cases where a vertical section of sea bed was encountered, video footage from the forward-looking wide-angle camera (Atlas, Insite Tritech Inc.) was examined instead. Over 100 h of video were watched to identify and georeference megabenthic invertebrate organisms larger than 10 mm. As identification to species level could not always be achieved, morphospecies (visually distinct taxa) were used for the analysis. High-resolution stills (Scorpio, Insite Tritech Inc., 2048 × 1536 pixels) and specimens were also collected to help with identifications. The position of each individual animal on the sea floor was determined using the ROV's ultra-short baseline navigation system (USBL). Substratum type (soft, hard or mixed sediments as well as live coral or rubble)

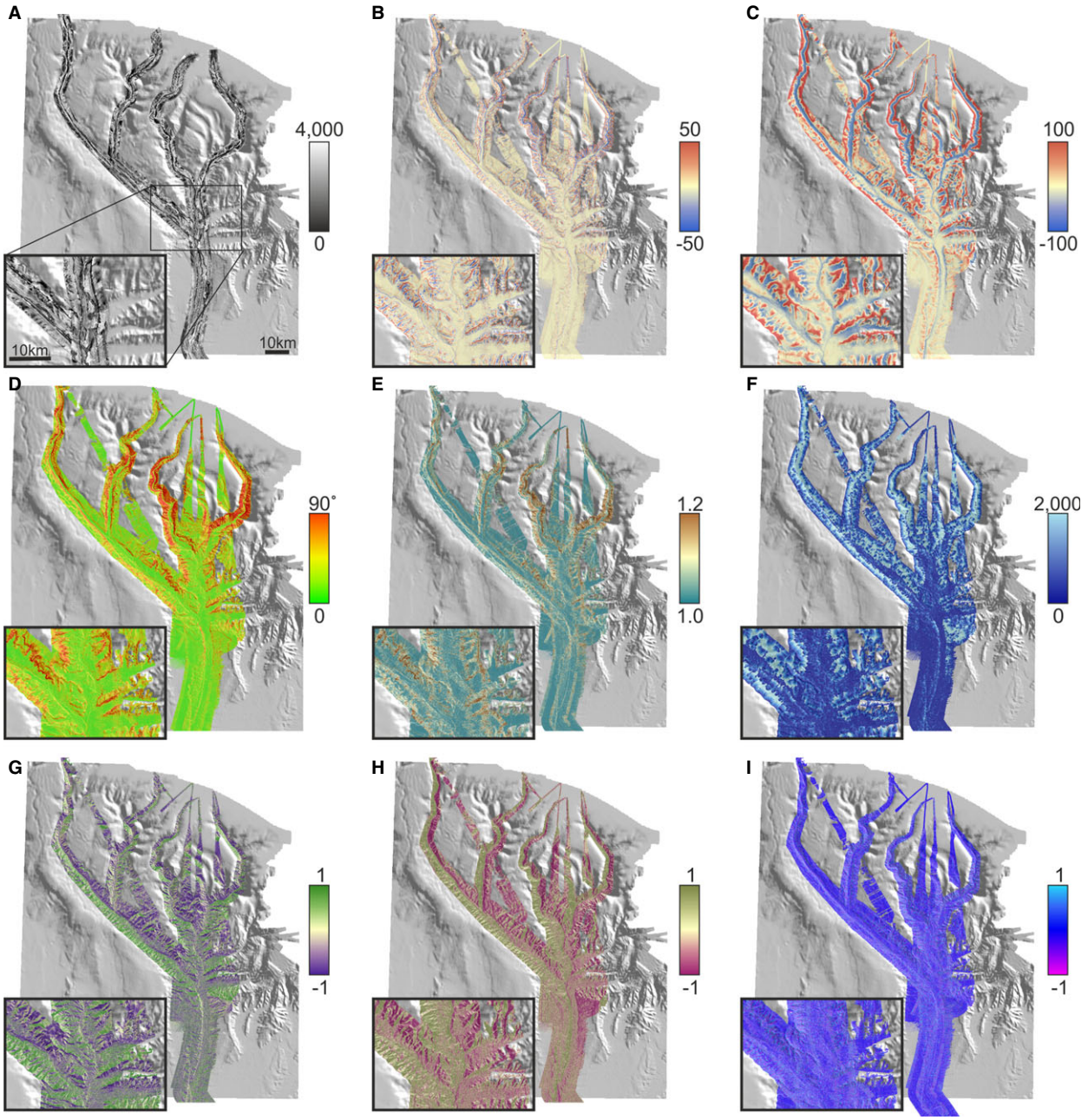

Fig. 2. Environmental variables (50 m resolution) derived from the acoustic survey. (A): sidescan backscatter (low backscatter in dark), (B): bathymetric position index (BPI) with neighbourhood of 500 m, (C): BPI with neighbourhood of 2 km, (D): slope (°); (E): surface area ratio, (F): downstream flow length, (G): northness, (H): eastness, (I): plan curvature. Background bathymetry (201 m resolution) provided by the Geological Survey of Ireland (Dublin).

and terrain inclination gradient (flat, sloping, vertical or complex) were also recorded. Distances travelled within each of these patches were measured. Two lasers representing 10 cm on the sea bed were present for scaling. A frame was extracted every minute (representing a 5 m displacement) using QUICKTIME 7 PRO (Apple Inc.) and the distance separating the scaling lasers was measured in the image processing software IMAGEJ (http://rsbweb.nih.gov/ij/). These measurements were used to standardize transect widths to 2.5 m.

Transects were subdivided into segments of 50 m in length and the species records consolidated. However, as the topography of Whittard Canyon varied greatly, the distance between the geographical co-ordinates of two

Table 1. Description and biological information for the 13 benthic video transects collected using the ROV *ISIS* and the four collected by *Genesis* for external model assessment. For biological characteristics, means based on 50-m sections are shown in parentheses.

Cruise	Dive	Branch	2D length (km)	3D length (km)	Mean depth (m)	SD depth (m)	Mean slope (°)	Video duration HH:MM:SS	No. individuals	Species richness	Simpson's reciprocal index
JC-010	063	Lower	1.60	1.68	−3868.7	120.0	28.7	05:19:22	352 (10.3)	17 (2.32)	2.55 (1.74)
JC-010	064	Eastern	4.13	4.39	−2959.7	341.4	32.5	08:25:35	1386 (15.7)	21 (1.35)	3.23 (0.96)
JC-010	065	Eastern	7.17	7.17	−1432.3	690.5	45.3	14:30:36	13134 (85.8)	73 (5.08)	6.32 (2.23)
JC-036	099	Western	3.15	3.24	−3638.3	254.0	17.8	09:55:43	125 (1.9)	13 (1.24)	1.77 (1.18)
JC-036	100	Western	2.93	3.01	−3396.2	389.0	19.4	08:58:18	325 (5.3)	35 (3.26)	9.15 (2.68)
JC-036	102	Western	1.94	2.04	−3095.9	232.5	26.7	06:46:06	335 (8.2)	24 (2.85)	4.34 (1.81)
JC-036	105	Western	1.60	1.73	−2550.1	521.6	36.6	07:00:30	2095 (56.6)	41 (3.89)	6.75 (2.01)
JC-036	107	Western	2.45	2.45	−778.2	170.4	27.3	09:49:48	1350 (26.5)	27 (2.67)	3.03 (1.80)
JC-036	109	Western	2.09	2.09	−1123.6	243.6	46.4	08:30:52	1287 (28.5)	60 (6.89)	8.36 (3.41)
JC-036	113	Eastern	2.09	2.35	−2334.2	1189.4	47.5	09:08:10	2270 (48.3)	33 (2.79)	2.64 (1.47)
JC-036	114	Eastern	1.50	1.64	−1462.1	164.4	39.0	11:21:54	9571 (290.0)	67 (9.97)	1.54 (2.68)
JC-036	115	Eastern	1.65	1.69	−1409.5	414.7	19.7	06:07:30	235 (6.9)	27 (2.32)	8.83 (1.76)
JC-036	116	Eastern	2.08	2.38	−1235.4	186.6	52.3	08:59:23	7399 (160.8)	52 (6.28)	4.24 (2.50)
JC-036	117	Eastern	2.34	2.67	−2199.2	188.3	51.9	11:00:46	3414 (63.2)	49 (4.85)	3.87 (2.21)
B-10/17b	003	Inner	3.89	4.03	−821.8	105.6	16.0	03:57:28	11856 (146.4)	24 (5.00)	2.04 (1.81)
B-10/17b	004	Inner	2.45	2.47	−922.8	83.2	9.5	02:24:32	9563 (191.3)	37 (5.48)	3.03 (2.11)
B-10/17b	005	Inner	1.39	1.42	−943.6	79.9	13.2	00:51:08	1352 (48.3)	14 (4.93)	2.9 (2.30)
B-10/17b	006	Inner	1.88	1.99	−746.3	186.5	19.0	01:57:34	2251 (56.3)	25 (2.93)	1.9 (1.42)

points would not accurately depict their three-dimensional (3D) separation. The vertical dimension was taken into account in ARCMAP 10 by using the 'Add Surface Information' tool in the '3D Analyst Toolbox'. This tool calculates the distance between two points based on the topography of a surface. Using the bathymetry raster as the input surface, the transects were separated into 50-m sections that took into account sea-bed topography. Differences between the lengths of 2D and 3D transects are reported in Table 1. Abundance, species richness and Simpson's reciprocal index (1/D,((Simpson 1949) were calculated for each transect and 50-m section. This index was chosen because it is more sensitive to changes in dominant species, whereas the importance of rare species is captured by species richness (Hill 1973). Components of beta diversity, a' (percentage of species occurring in both a focal and neighbour sample), b' (percentage of species occurring in focal sample but not in neighbour sample) and c' (percentage of species occurring in neighbour sample but not in focal one) were also calculated between ROV dives (Koleff *et al.* 2003).

Predictive modelling

General additive models (GAMs)

General additive models (GAMs) are similar to general linear models (GLMs) in that they allow the building of models with different error structures and link functions, but they are not limited to modelling relationships for which the form is known *a priori* (Crawley 2007). Instead, they make use of non-parametric smoothers, such as regression splines or tensor products, which allows for the building of more complex (*e.g.* non-linear, non-monotonic) relationships (Guisan *et al.* 2002). GAMs have the potential to explain additional variation, as compared to GLMs. However, consideration must be given to the appropriate level of smoothing to avoid over-fitting (Wood & Augustin 2002).

General additive models were used to build predictive maps for each of the biological characteristics calculated (abundance, species richness, Simpson's reciprocal index and cold-water coral presence). Abundance was log + 1 transformed prior to modelling to improve normality and was modelled using normally distributed errors. The Simpson's reciprocal index was also modelled using normally distributed errors. In the case of species richness, as the data were only composed of positive integers, a Poisson distribution was used whereas presence−absence of cold-water coral colonies was modelled using a binomial distribution. For coral presence, only colonial, framework-building scleractinians were considered (*Madrepora oculata*, *Lophelia pertusa* and *Solenosmilia variabilis*), as they can be considered habitat-forming species. Environmental variables were assessed by forward selection; the variables resulting in the highest deviance explained were added one step at a time until no more statistically significant (P-value < 0.05) variables could be added. The significance of the addition was assessed by comparing the

reduction in deviance caused by the additional variable in comparison to the previous model using the χ^2 statistics (Guisan *et al.* 2002). Using the most parsimonious models, full coverage maps were created by predicting values for each pixel of the bathymetry. To avoid rescaling nonlinear relationships, such as diversity−area, the pixels show the expected value for a section of sea bed of the same area as sampled, *i.e.* 2.5 × 50 m or 125 m^2. A measure of prediction variability was generated by mapping the SE associated with the expected value for each pixel.

Spatial correlograms, using Moran's I index of spatial autocorrelation (Legendre & Fortin 1989), of the 50-m sections data set suggested that most of the spatial autocorrelation present occurred at scales <100 m, except for cold-water coral presence, which occurs at <50 m (results shown in Supporting Information S1). As such, the 50-m sections were systematically subsampled to create distances of at least 100 m, resulting in half the data set being considered for model building (similar results were obtained using either set of subsamples), except in the case of coral presence, for which subsampling was not carried out. The 50-m sections not used for model building were subsequently employed for model assessment. Statistical analyses were carried out using the statistical package R (R Development Core Team 2011) and the library 'mgcv'.

Random forest (RF)

Random forest (RF) is a technique whereby multiple decision trees are built based on random subsamples of the data and the environmental predictors, leading to the construction of a 'forest' (Breiman 2001). Trees are built by binary splits such that the data are recursively separated into smaller and smaller groupings based on the best predictor variable available. As each tree will be built based on a different set of samples and environmental predictors, each tree will be different and once grown can be used to make predictions based on the rules developed at each node (Cutler *et al.* 2007). Each tree provides an answer and the average (in the regressive case) is the expected value.

For each of the biological characteristics measured, a total of 1000 trees were built with 12 variables being randomly selected at each node. Full coverage maps were obtained by making predictions for each pixel of the bathymetry and uncertainty maps were calculated by taking the SD of the 1000 predicted values (one from each tree) for each pixel. Variable importance was measured using the out-of-bag (OOB) data, the part of the randomly subsampled data not used for building the tree. As values for the OOB data are known, a measure of accuracy (the mean squared error) can be obtained by comparing the known values with the estimates obtained when these samples are regressed along the trees (Hastie *et al.* 2009). Each predictor variable is then permuted, the accuracy measure recomputed and the mean difference averaged over all trees. The same data set as for the GAMs was used and functions from the R package 'randomForest' were employed.

Model comparison

The performance of each model was assessed by calculating the amount of variation explained when the predicted values were regressed against the known values from the 50-m sections that had not been used to build the models. The root-mean-square error (RMSE) was also calculated to give a more easily comparable measure between the observed and predicted values (Knudby *et al.* 2010). However, as previous work suggested that split-sample assessment methods may yield overly optimistic results (Araújo *et al.* 2005; Randin *et al.* 2006), comparisons with an independently collected data set were also carried out. This data set was comprised of four ROV video transects collected using the 1400 m-rated inspection-class sub-Atlantic Cherokee ROV *Genesis* on board the RV *Belgica* during the 2010 cruise 10/17b. These transects (B10-03, B10-04, B10-05 and B10-06) were acquired at an average speed of ~0.3 $m \cdot s^{-1}$ using four video cameras (including forward looking) and a digital Canon Powershot colour stills camera (250 W Q-LED illumination) and were located in the two inner branches of the canyon (Fig. 1). Two parallel laser beams with a distance of 10 cm were used as a scale during sea-bed observations, and the sea-bed positioning was recorded using the IXSEA USBL Global Acoustic Positioning System (GAPS) system. These transects were analysed in the same manner as the ROV *ISIS* video transects. Using subsections of 50 m, the results obtained were regressed against the values predicted by the different models and the RMSE was calculated.

Vertical structures

As an association between vertical walls and high biodiversity was known for Whittard Canyon (Huvenne *et al.* 2011; Johnson *et al.* 2013), areas with slopes >35° were selected and polygons representing individual steep vertical walls were created. Owing to the depths surveyed, the coarser ship-board bathymetry resolution causes slope values to be underestimated. Based on the imagery available, slopes >35° could potentially represent near-vertical walls (Huvenne *et al.* 2011). Pixels predicted to be in the top 90% for at least four of the maps created for abundance, species richness or Simpson's reciprocal index for either GAMs or RF were identified. These selected pixels represented areas likely to harbour diverse communities

with high abundances. The number of such pixels found within each polygon was calculated and standardized based on the surface area of the polygon. The same was carried out for pixels that showed high suitability for presence of corals (0.6 for GAMs and 0.8 for RF).

Results

A wide variety of sea-bed environments were observed within Whittard Canyon (Fig. 3) with a median substratum patch size <100 m and beta diversity measures indicating that only a relatively small percentage of species (<40%) tended to be shared between transects (results are shown in Supporting Information S2). The high turnover in species assemblages is one of the main reasons this study focused on biological characteristics as opposed to specific species assemblages. A total of 42,934 individuals and 202 morphospecies were observed in the initial *JC* survey, with the most commonly observed taxa (representing ~60% of individuals) being xenophyophores (probably *Syringammina fragilissima*), *Pentametrocrinus* sp., *Acanella* sp., *Lophelia pertusa*, cerianthids and

Fig. 3. Example images of environments encountered and organisms observed. (A): hummocky sediment, (B): rocky outcrop, (C): exposed bedrock with single coral colony, (D): burrowed wall with cerianthids, (E): steep gully with brisingids, (F): vertical wall with *Primnoa* and *Solenosmilia variabilis*, (G): soft sediments with *Acanella* sp., (H): rocky outcrop with cormatulids, (I): stylasterid coral and associated community, (J): soft sediments with Pennatulacea and *Pentametrocrinus* sp., (K): vertical wall with *Anthomastus* sp. and brisingids, (L): vertical wall with *Lophelia pertusa*, *Acesta* sp., *Actinauge* sp. and comatulids. Scale bars = 10 cm.

Anthomastus sp. The eastern and western branch harboured similar numbers of species, but abundance was much greater in the eastern branch (on average 82 individuals per 50-m section compared with 17). A greater percentage of the western branch was composed of flat, soft sediment (82% *versus* 53%) and deposit feeders were more common in this branch. In shallower (<1000 m) and deeper transects (>3800 m), cerianthids dominated the observations. Holothurians and ophiuroids increased in relative abundance at 2700−3700 m depth, with the former composing a greater percentage of observations in the western branch. Soft corals, particularly *Acanella* (or possibly *Chrysogorgia*) and *Anthomastus*, were predominant at 1500−3500 m in depth, particularly in more morphologically complex areas. Stalked crinoids appeared to be more frequent on hard bottoms whereas *Pentametrocrinus* was frequently observed in flat areas. Xenophyophores composed a large portion of observations in flat, soft sediments at 1200 m.

In total, 58 morphospecies and 25,022 individuals were observed in the four transects of the *Belgica* cruise 10/17b, of which eight morphospecies had not been recorded in the previous survey. In these transects, the most commonly observed morphospecies were cerianthids, *Kophobelemnon*, and *Madrepora oculata* (representing ~80% of individuals). Although the majority of the morphospecies observed in the *Belgica* transects had been observed during the previous cruises, their relative composition differed. Soft corals, possibly owing to the shallower transect depths, were not as frequently observed throughout the inner canyon branches. Instead echinoids (*Cidaris cidaris* and *Phormosoma placenta*), sea pens (*Kophobelemnon*) and cerianthids were more prevalent. Large aggregations of sea pens (particularly *Kophobelemnon* sp., but also *Pennatula aculeata*) were observed, at depths of 800−900 m and 900−1000 m, respectively, in areas dominated by soft sediments. Sea pen meadows composed of *Pennatula* sp. have been reported for submarine canyons of the western Atlantic (Baker *et al.* 2012), and of *Kophobelemnon* sp. in other canyons of the Bay of Biscay (Davies *et al.* 2014). Few instances of areas dominated by mixed or hard sediments were recorded for the *Belgica* transects, but areas dominated by coral rubble or live corals in flat areas were more prevalent. Detailed species composition by dive, depth section and substratum type are presented in Supporting information S3−S5. When available, a representative image for each observed morphospecies was deposited in the online media archive of the SERPENT project (http://archive.serpentproject.com/view/sites/sea_14.html).

Transect lengths differed between dives (Table 1), with dive *JC*-065 being the longest and the one with the overall highest abundance and species richness. However, the highest diversity at the transect level was observed in dives *JC*-100, *JC*-115 and *JC*-109. When averages based on the 50-m sections were compared instead, dives *JC*-114 and *JC*-116 had the highest abundance, species richness (with dive *JC*-109) and diversity as measured by Simpson's reciprocal index (with dives *JC*-100 and *JC*-109). Lowest abundance and species richness were found in dive *JC*-099 with low diversities (1/D), based on averaged 50-m sections, in dive *JC*-064. With dive *B*10-05, these transects represented those having the highest percentages of soft sediments in flat areas.

In both GAMs and RF, depth was the most important environmental variable for predicting abundance (Figs 4 and 5). Although a general decrease in abundance with depth was observed, peaks occurred at ~1200, 2200, 3000 and 3700 m. Coarse-scale BPI (2 km) indicated that lower abundances could be expected in flat regions and a similar trend was observed for curvature. Steeper slopes were expected to have higher abundances and although not selected by GAMs, RF also found surface area ratio to be a useful predictor. Downstream flow length indicated a general decrease in abundance towards the canyon thalweg. Differences in prediction extent between certain models were caused by the smaller extent of the TOBI backscatter layer.

As for abundance, depth and slope were also significant predictors of species richness in both GAMs and RF. An overall negative relationship with depth was observed, with the highest species richness recorded at 1200 m, whereas steep slopes (>20°) had a positive effect (Figs 4 and 6). Higher species richness was characteristic of regions with high SDs of slope, but a lower number of species was expected on strongly east- or west-facing slopes. Coarse scale BPIs (1 and 2 km) were good predictors in both GAMs and RF, and indicated lower species richness in flat areas, a trend also supported by the relationship observed with general curvature. The canyon thalweg also harboured lower species richness as indicated by the relationship with the downstream flow length and the decrease in species richness in low backscatter areas.

For Simpson's reciprocal index, coarse scale BPIs (2 or 1 km) were more significant than either depth or slope in both GAMs and RF (Figs 4 and 7). As for abundance and species richness, lower biodiversity was found in flat areas and a positive relationship with slope was observed. Although not selected by GAMs, RF also found depth to be important in predicting biodiversity. The relationship to plan curvature suggests that very fine-scale ridges may harbour higher diversity (1/D) than valleys.

Three species of colony-forming cold-water corals were observed: *Madrepora oculata* (39 colonies), *Lophelia pertusa* (3337 colonies) and *Solenosmilia variabilis* (383 colonies). Dive *JC*-116 in the eastern branch imaged the 120-m-high coral wall mapped by Huvenne *et al.*

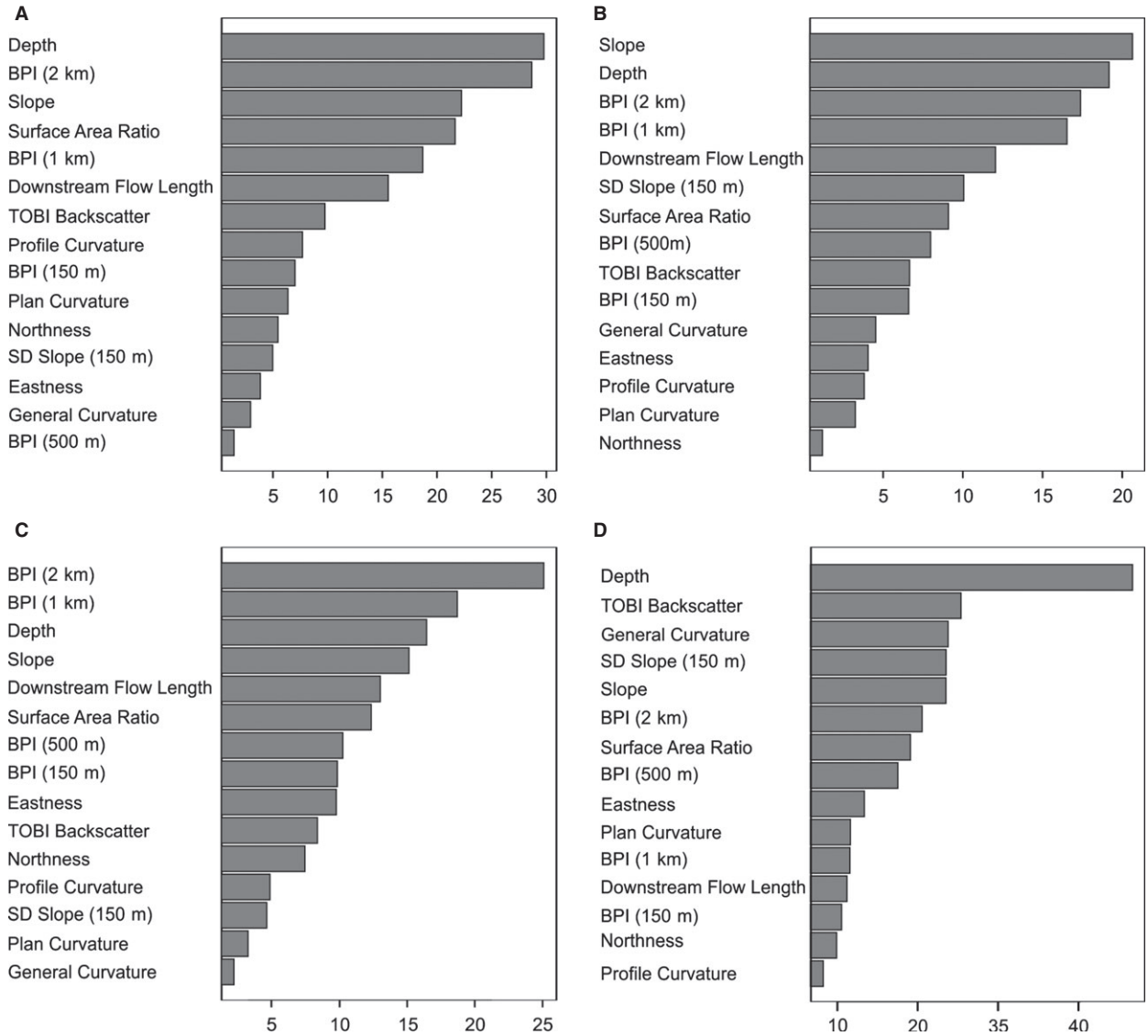

Fig. 4. Variable importance (reported as percentage increase in mean squared errors) for the random forest models for (A): abundance, (B): species richness, (C): Simpson's reciprocal index, (D): cold-water coral presence. BPI, bathymetric position index; TOBI, towed ocean bottom instrument.

(2011), whereas a smaller, sparser and less diverse coral wall was also found in the western branch during dive *JC*-109. Presence of cold-water coral was predicted in association with finer-scale variations in sea-bed morphology, with fine-scale BPI (150 m) being the first predictor selected by GAMs (Fig. 8). RF also found fine-scale descriptors to be of greater importance than for the previous biological characteristics, with the SD of slope and general curvature as most useful (Fig. 4). Cold-water corals were more likely to occur in areas of complex topography with higher rugosity as opposed to flatter areas. This was also apparent at the coarser scale as shown by the BPI (2 km) and the sharp decrease in coral presence towards the canyon thalweg. RF also highlighted the importance of depth and slope. Both RF and GAMs found TOBI backscatter to be a useful predictor of cold-water coral presence; the relationship identified by GAMs indicates a higher likelihood of coral presence in areas characterized by higher TOBI backscatter, which is indicative of hard substratum.

In the case of abundance, uncertainty (Fig. 5B and D) was highest in shallower and deeper sections of the canyons past the limit of the available data. Higher variability in the predictions of species richness (Fig. 6B and D) and Simpson's reciprocal index (Fig. 7B and D) was observed in association with the canyon walls in elevated areas characterized by steep slopes. Higher overall variability was typically observed for RF predictions.

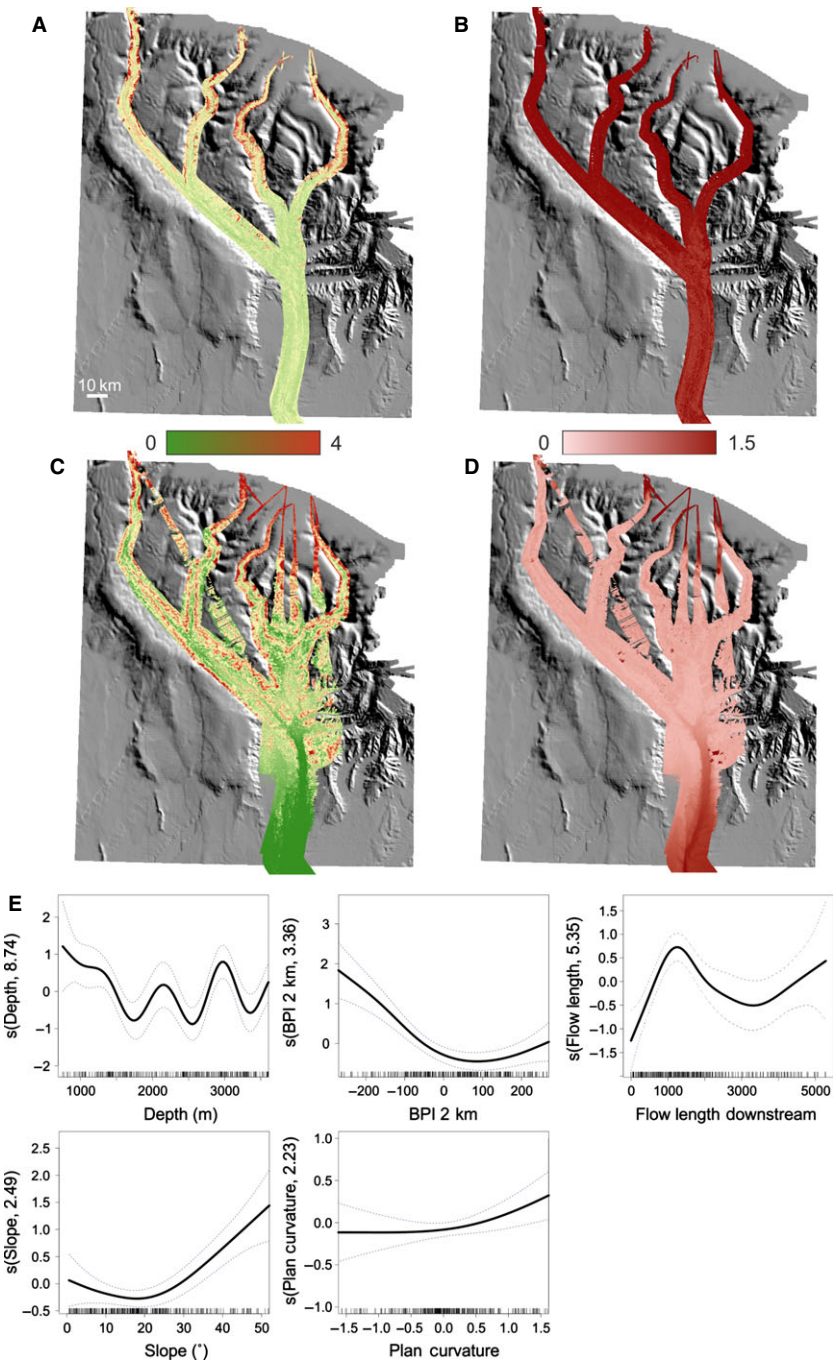

Fig. 5. Model output for predicting abundances within a 125-m^2 section of sea bed across the extent of the survey. (A): random forest prediction map and (B): uncertainty map, (C): general additive model (GAM) prediction map and (D): uncertainty map. Abundance prediction map represents log+1 transformed data. (E): Relationship (centred smooth component and its estimated degrees of freedoms, black line) for the selected environmental variables using GAMs with the dashed lines representing the SE estimated for the predictions. Background bathymetry (201 m resolution) provided by the Geological Survey of Ireland (Dublin). BPI, bathymetric position index.

Overall, GAMs appeared better able to model the biological characteristics of interest using the available environmental variables (Table 2). GAMs were able to explain 59.3% of the variation in species richness, 43.2% in abundance and 29.7% of Simpson's reciprocal index, compared with 30.6%, 33.1% and 23.4% when RF were considered. However, RF consistently scored higher than GAMs when the removed portion of the data set was compared. When a completely independent data set was used, models for abundance and Simpson's reciprocal index were only able to explain a small percentage of the variation observed whereas the model for species richness was not significant. Differences in relative species composition were apparent (Supporting Information S2 and S3) and may in part result from the shallower depths (depths for which highest abundances and species richness were

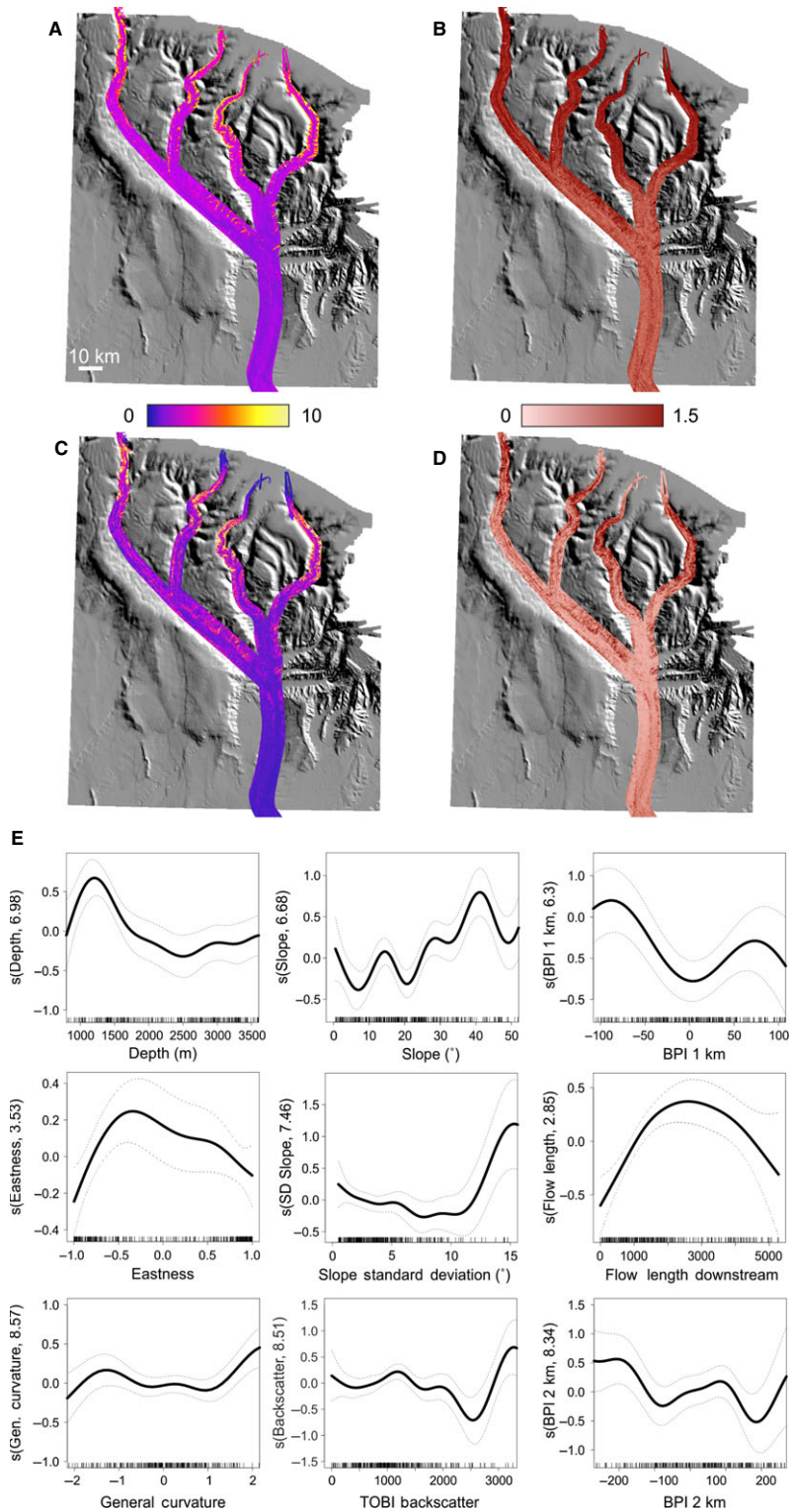

Fig. 6. Model output for predicting species richness within a 125-m^2 section of sea bed across the extent of the survey. (A): random forest prediction map and (B): uncertainty map, (C): general additive model (GAM) prediction map and (D): uncertainty map. (E) Relationship (centred smooth component and its estimated degrees of freedoms, black line) for the selected environmental variables using GAMs with the dashed lines representing the SE estimated for the predictions. Background bathymetry (201 m resolution) provided by the Geological Survey of Ireland (Dublin). BPI, bathymetric position index; TOBI, towed ocean bottom instrument.

recorded during the *JC* cruises were not sampled during the *Belgica* cruise) and relative differences in substratum type encountered in the two inner branches. Accuracy measures for the prediction of cold-water coral presence indicated that RF outperformed GAMs, obtaining values of 71.4% as opposed to only 65.3%. RMSE values indicated a clear difference between the methods of model assessment, with the use of an external data set

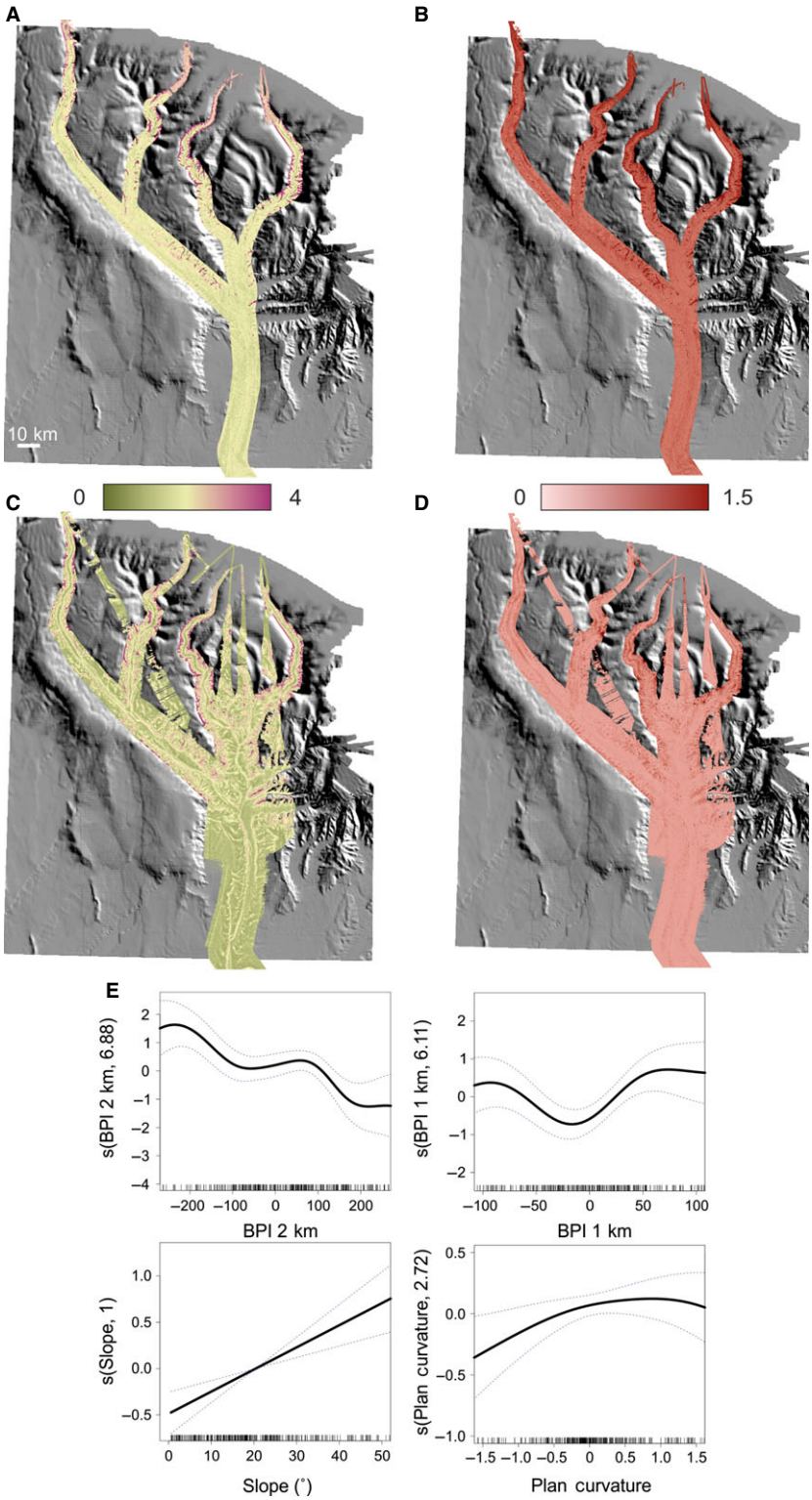

Fig. 7. Model output for predicting Simpson's reciprocal index (1/D) within a 125-m^2 section of sea bed across the extent of the survey. (A): random forest prediction map and (B): uncertainty map, (C): general additive model (GAM) prediction map and (D): uncertainty map. (E): Relationship (centred smooth component and its estimated degrees of freedoms, black line) for the selected environmental variables using GAMs with the dashed lines representing the SE estimated for the predictions. Background bathymetry (201 m resolution) provided by the Geological Survey of Ireland (Dublin). BPI, bathymetric position index.

consistently showing greater deviations from predicted values (Fig. 9). Model agreement between GAMs and RF varied around ~55%, with the most similar model produced for species richness, with a 64.3% agreement, when values at the position of the data points used to build the models were compared. When the predictions

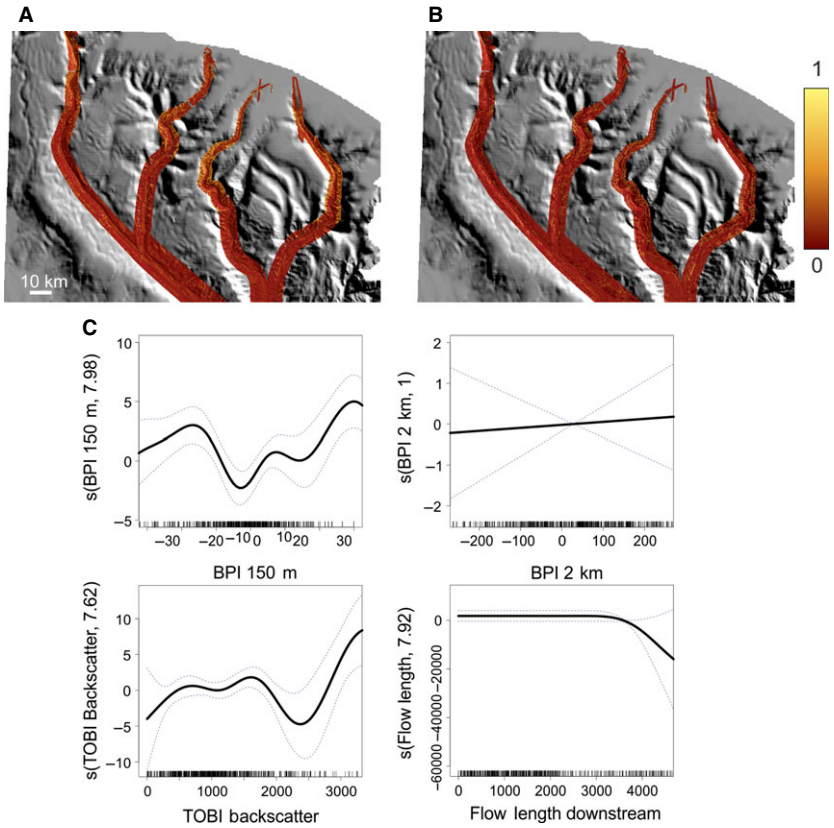

Fig. 8. Model output for predicting the presence of scleractinian corals within a 125-m^2 section of sea bed across the extent of the survey. (A): random forest prediction map and (B): general additive model (GAM) prediction map. (C): Relationship (centred smooth component and its estimated degrees of freedoms, black line) for the selected environmental variables using GAMs with the dashed lines representing the SE estimated for the predictions. Background bathymetry (201 m resolution) provided by the Geological Survey of Ireland (Dublin). BPI, bathymetric position index; TOBI, towed ocean bottom instrument.

for the entirety of the canyon were compared, model agreement fell to ~30% with the highest agreement for diversity at 40%. Although coral presence was found to have the highest percentages of deviance (GAMs) and variance (RF) explained, 59.8% and 41.0%, respectively, agreement between the two models was lowest at just 17.7% for the sampled locations.

When finer-scale environmental information was incorporated into the model (identified from the video data), performance was increased by an additional 16.9% and 13.5% for GAMs and RF, respectively, in the case of abundance, and 3.4% and 8.7% in the case of species richness (Table 2). Fine-scale substratum and terrain gradient did not appear to help model Simpson's reciprocal index. The highest abundance and species richness were found in areas of vertical walls covered by the cold-water coral *Lophelia pertusa* (Fig. 10). In these 50-m sections, average abundances of 734 individuals and 15 different morphospecies were recorded.

Only 33.4 km^2 (representing 0.52% of the 3D area of canyon surveyed) of sea bed in the Whittard Canyon was likely to have vertical walls and only a total of 9.4 km^2 of sea bed or 0.15% had vertical walls shallower than 2000 m in depth where colonial cold-water corals were likely to occur. However, even fewer vertical areas were identified as probably harbouring high abundances, species richness or diversity (1/D), and even more rarely to be suitable for coral growth (Fig. 11). These respectively represent 11.2 km^2 or 0.17% (4.3 km^2 or 0.07% shallower than 2000 m depth) and 1.5 km^2 or 0.02%.

Discussion

Although submarine canyons are numerous [Harris & Whiteway (2011) identified over 5800 large canyons worldwide], very few have been mapped to high resolutions and even fewer attempts have been made to build full coverage biological maps. Both GAMs and RF, although predictions differed, were able to produce useful predictive maps for abundance, species richness, Simpson's reciprocal index and cold-water coral presence. Such differences in predictions between different models are not unexpected (Araújo & New 2007; Palialexis *et al.* 2011), and consideration of both model outputs is necessary when building ensemble predictions that can strengthen conclusions.

Whittard Canyon processes and ecology

The environmental parameters selected as most useful in modelling abundance, species richness and diversity (1/D)

Table 2. Model performances in percentages. Values reported represent deviation explained for general additive models (GAMs) and variation explained for random forest (RF), except for the evaluation of cold-water coral presence against independent data, which represents measures of accuracy. For the modelled data, percentages in parentheses represent the additional variance explained when fine-scale environmental variables extracted from the imagery were also considered. For model agreement the first value is the percentage agreement when only values at sampled locations were compared, whereas the percentages in parentheses represent a comparison using the entire extent of the prediction maps.

	Model performance (%)			
	Modelled data	Split-sample data	Independent data	Model agreement
Abundance				
GAM	43.2 (16.9)	33.2	4.3	56.1 (29.3)
RF	33.1 (13.5)	40.9	11.1	
Species richness				
GAM	59.3 (3.4)	31.5	NS	64.3 (31.0)
RF	30.6 (8.7)	39.9	NS	
Simpson's reciprocal index				
GAM	29.7 (0.7)	15.4	14.3	54.8 (40.0)
RF	23.4 (1.8)	29	9.4	
Coral presence				
GAM	59.8	NA	65.3	17.7 (4.5)
RF	41.0	NA	71.4	

NA, Not applicable; NS, Not significant.

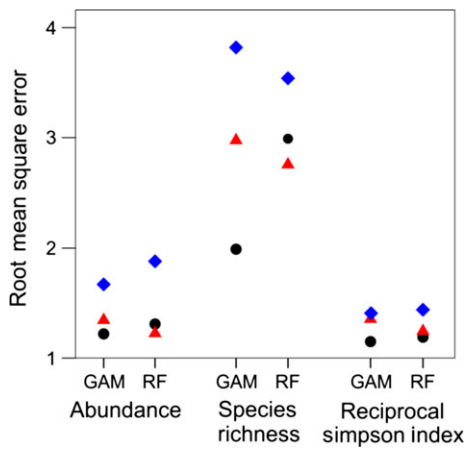

Fig. 9. Root-mean-square-error for the different types of model assessment: modelled data (black circles), split-sample data (red triangles) and independent data (blue diamonds). GAM, general additive model; RF, random forest.

support what is currently known of the ecology of submarine canyons and cold-water corals. The morphology of Whittard Canyon combined with water-mass properties and dominant currents within the Bay of Biscay indicated that our predictive maps are consistent with spatial patterns documented for other submarine canyons in this region.

Deep-sea organisms are mostly reliant on the flux of organic material from the sunlit surface waters, which decreases exponentially with depth (Lutz *et al.* 2007). Although the complexity of canyons and their role in channelling material from the continental shelf may create significant variations in the spatial trends observed, decreases in abundance or species richness from a canyon's mid-slope towards the abyssal plain have been observed (Currie & Sorokin 2014; Duffy *et al.* 2014; Frutos & Sorbe 2014). In this study, depth (or other unmeasured co-varying environmental factors) appeared as a particularly strong predictor for both megafaunal abundance and species richness. Within Whittard Canyon a general decrease in organic content with depth has previously been found, but with the canyon floor showing local enrichment as compared with the nearby slope (Duineveld *et al.* 2001).

The highest species richness in Whittard Canyon was found between 1200−1300 m at a large coral wall dominated by *Lophelia pertusa*. These observations coincided with bottom nepheloid layers (1200−2000 m in depth) and increased suspended particulate organic matter (Huvenne *et al.* 2011). These nepheloid layers are related to the interface between the Mediterranean Outflow Water (MOW), a slightly warmer and more saline water mass that originates as a density-driven overflow and flows northward along the continental slope past the Celtic Margin and Porcupine Bank, and the lower salinity Labrador Sea Water (van Aken 2000). The interface between these layers may result in locally focussed hydrodynamic processes such as internal waves, which may help keep organic matter in suspension, creating an enhanced food supply for the coral colonies (Mienis *et al.* 2007). This increased food supply may also propagate downslope and help explain why the highest density of corals found in Whittard Canyon (Huvenne *et al.* 2011) was located deeper than the potential density envelope suggested to be optimal for coral growth in the Northeast Atlantic (Dullo *et al.* 2008). Increased flow velocities were also associated with an increase in the density of filter feeders along the slope of the nearby Goban Spur at 1000−1500 m in depth (Flach *et al.* 1998). Similarly, dense assemblages of oysters, *Neopycnodonte zibrowii*, were found in association with the shallower (~500−800 m) interface of the Eastern North Atlantic Water and the MOW in a different branch of Whittard Canyon (Johnson *et al.* 2013), and in another canyon of the Bay of Biscay (Van Rooij *et al.* 2010a).

In addition to keeping food in suspension, it is suggested that the hydrodynamic regime of the Bay of Biscay has resulted in erosional features characterized by

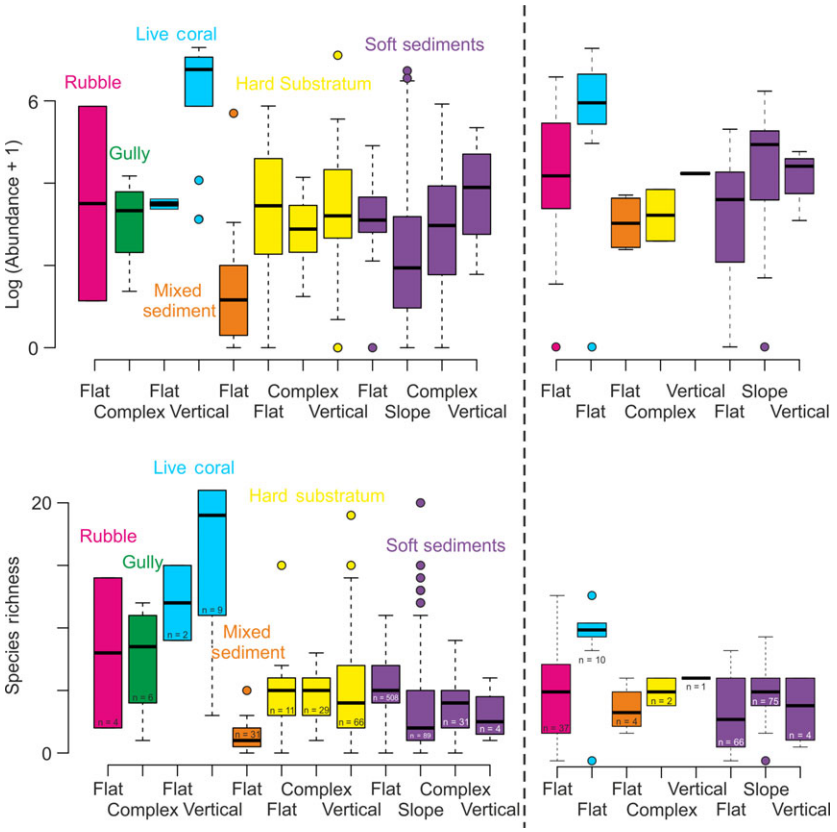

Fig. 10. Boxplot of abundance and species richness as observed for different substratum types and terrain gradients: ROV *ISIS* transects (left) and ROV *Genesis* (right). The number (n) of 50-m sections from each substratum type is shown.

step-like banks with walls of hard substratum suitable for attachment (Van Rooij *et al.* 2010a). The MOW flowing from east to west affects the morphology of the sea bed with the eastern flank receiving higher sediment deposition whereas the western flank acts as an obstacle that intensifies bottom current and leads to increased erosion (Van Rooij *et al.* 2010b). Comparable step-like features were visible in portions of the east-facing coral wall found along dive *JC*-116 on the western flank of the eastern canyon branch. Similar patterns have been observed for cold-water coral occurrences in Penmarc'h, Guilvinec (De Mol *et al.* 2011), Dangeard and Explorer canyons (Stewart *et al.* 2014) of the Bay of Biscay, whereas *Lophelia pertusa* frameworks were also associated with vertical cliffs in the Lacaze-Duthiers canyon, northwestern Mediterranean (Gori *et al.* 2013). *Solenosmilia variabilis* was also observed in the *Lophelia pertusa*-dominated wall, but was also found to occur deeper (up to 1850 m).

All biological characteristics measured in this study decreased towards the thalweg. As indicated by the relationships with BPI, SD of slope and curvature, this decrease towards the thalweg may result from a reduction in habitat complexity. As opposed to the more morphologically diverse canyon walls, where overhangs and gullies were observed, the thalweg was, for the most part, characterized by flat areas of soft sediment. High numbers of cenrianthids, ophiuroids and *Acanella* sp. were sometimes observed in flat sediment areas, but diversity remained low. Of course, this analysis focused on epibenthic megafauna, and patterns in the infauna may show very different trends. However, macrofaunal abundance and biomass in Whittard Canyon decreases with depth, with their composition changing with respect to the relative abundance of different feeding types (Duineveld *et al.* 2001). Positive associations with topographic variability, as measured by fine-scale BPI, SD of slope or rugosity, have been reported for cold-water coral occurrences (Henry *et al.* 2010; Rengstorf *et al.* 2013), and these variables have also been found to help explain benthic community composition (Jones & Brewer 2012; Henry *et al.* 2013). More frequent disturbances within the canyon's thalweg owing to density flows or turbidity currents could also explain the reduced diversity. Similarly, they could also explain the reduced species richness found at shallower depths towards the head of the canyon where more physical activity could be occurring. Patterns of reduced diversity, although mediated by productivity, have been recorded for polychaetes in areas of canyons

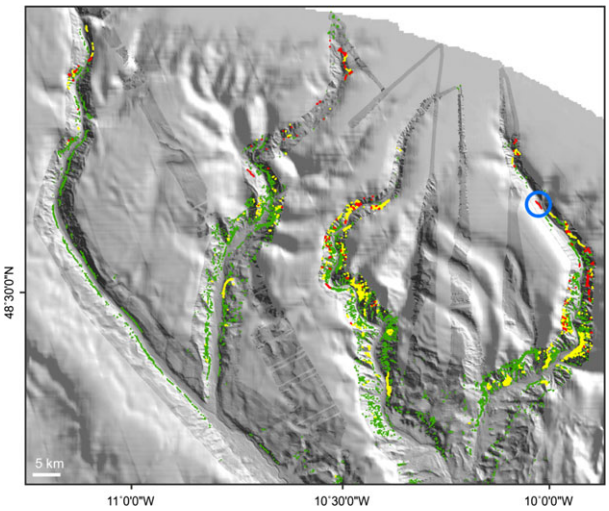

Fig. 11. Maps of steep slope areas (slopes of >35°, representing near-vertical walls, green) for which general additive models and random forest models indicated a high combined potential for abundance, species richness and/or diversity (1/D) (yellow) or cold-water corals (red). The blue circle represents the location of the vertical wall colonized by *Lophelia pertusa* and imaged during the *JC* -035-036 cruises. Background bathymetry (201 m resolution) provided by the Geological Survey of Ireland (Dublin).

characterized by frequent disturbances (Paterson *et al.* 2011). Lowered infaunal species diversities have also been found at the head of the active La Jolla canyon (Vetter & Dayton 1998).

Overall, the morphological complexity of the canyon has led to rich habitat diversity with high species turnover. Although no comparisons were carried out with transects on the continental slope, this high local variation appears to provide multiple niches, which would promote species co-existence and positively influence regional diversity. Although a few species appeared in multiple habitats (*Acanella* sp., *Anthomasthus* sp. and cerianthids, although species-level identification could not be achieved and may lead to further differentiations), many were restricted to a specific set of environmental conditions and very few transects were dominated by a single species. These most common taxa appeared in relatively wide depth bands. Similarly wide depth bands (800−2100 m) were found for *Anthoptilum*, *Anthomastus* and *Acanella* on the Mid-Atlantic Ridge (Mortensen *et al.* 2008).

At two distinct depth bands (700−1000 m and 3700−4000 m), cerianthids appeared to dominate the observations, suggesting that, although morphologically similar, at least two separate species probably occur within Whittard Canyon. At the deeper depths, cerianthids were observed buried in soft sediment, whereas along the shallower transects they were observed along a semi-lithified sediment wall. Along this transect, burrowing ophiuroids were also repeatedly observed, forming an assemblage similar to the one described for canyons of the South West Approaches, Northeast Atlantic (Davies *et al.* 2014). These authors also described *Kophobelemnon stelliferum*−cerianthid assemblages, in which high abundances of *Pentametrocrinus* and xenophyophores were also found. In the present study, *Kophobelemnon* and cerianthids were observed along the shallower transects carried out in the inner branches. *Syringammina fragilissima* was the dominant species along transect *JC*-114, at depths (1200 m) similar to where high densities of xenophyophores (probably *Syringammina* sp.) were also reported for the Gully canyon, Northwest Atlantic (Kenchington *et al.* 2014). This species has also been reported for the upper Nazaré canyon (1500 m), Northeast Atlantic, where they occur on steep sediment-covered slopes in areas of enhanced food fluxes (Gooday *et al.* 2011).

Within particular habitats the presence of certain species, such as cold-water corals, appeared to have a further influence on biological characteristics. Although the diversity of octocorals has been found to decrease in *Lophelia pertusa* reef environments (Morris *et al.* 2013), in the current study when all taxa were considered, vertical walls dominated by cold-water corals were found to have the highest diversity of all habitats observed. This may be the result of ecological facilitation whereby the 3D coral structure could provide attachment for a variety of sessile species, positively affect hydrodynamic patterns for filter feeders or provide a complex habitat affording protection against predation (Buhl-Mortensen & Mortensen 2004; Clark *et al.* 2008). By comparison with observations on the Mid-Atlantic Ridge and in many other cold-water coral areas, *Acesta excavata* and crinoids were found to associate with *Lophelia pertusa* (Mortensen *et al.* 2008). In addition, *Actinauge* sp., *Desmophyllum* sp., *Echinus* spp., *Gorgonocephalus* sp., *Geodia* spp. and various species of soft corals were commonly observed. These particularly rich and populated habitats may also help maintain the regional diversity by acting as sources to help colonize less suitable (sink) habitats (De Leo *et al.* 2014).

Assessment and limitations

As variations in bottom-water temperature, salinity and oxygen concentration within Whittard Canyon tend to co-vary with depth (Duros *et al.* 2011), the lack of fine-scale layers describing hydrographical conditions is not expected to be a major limitation of the present study. However, adding information on average current velocities or temperature and salinity across different water masses has been found to help explain the spatial patterns

of species in other studies (e.g. Henry *et al.* 2013). The bathymetry-derived environmental descriptors were able to explain a good percentage of the spatial variation observed in biological characteristics; still, a significant percentage remained unexplained and finer-scale information on current speeds in areas of internal waves or local variation in food supply may prove useful. Unfortunately, the information was not available at the appropriate fine scale for the entire canyon. Similarly, a detailed sea-floor sediment interpretation map was not available for Whittard Canyon. The increase in model performance obtained when imagery-derived environmental descriptors were included indicated that fine-scale substratum information would be valuable. Although sidescan sonar backscatter can be used as a proxy for sediment hardness, the complex morphology of the canyon sea floor affects the angle of incidence, and therefore backscatter strength. Although 'true slant range' correction was applied during processing, the backscatter was still visibly affected by sea-bed morphology, only providing a useful proxy for sediment hardness in flatter areas.

Presently, the spatial predictions presented represent only a snapshot in time, whereas spatial patterns may continue to change over time. Although temporal variability in submarine canyons can range from diurnal (Matabos *et al.* 2014) to seasonal (Juniper *et al.* 2013) to short- and long-term geological time scales, the major influence on abundance and species diversity observed in this study was associated with long-lived reef-building coral colonies. For the scale of this survey, no temporal differences were observed between the *ISIS* ROV surveys of 2007 and 2009. As such, the additional 1-year time difference with the externally collected data set (ROV *Genesis*) is unlikely to be the reason for the disparity in estimates. As mentioned before, the more plausible causes are the differences in depth and substratum composition.

With the current environmental information available, the statistical approach that produced the best predictions depended on the biological characteristic of interest. RF had been found to outperform many other statistical techniques including GAMs when predicting distributions of tree species (Marmion *et al.* 2009b), but comparable performances were obtained for butterflies (Marmion *et al.* 2009a). However, GAMs were found to be more successful in predicting fish abundance as opposed to RF, which performed better for species richness and diversity (Knudby *et al.* 2010). These authors attribute this difference to the binary splits of tree-based methods having more difficulties in predicting extreme values. As the results of RF do not lead to clear relationships between the response and the environmental variables, a more effective approach might be to use GAMs first for data exploration and variable selection and then to use RF for prediction (Baccini *et al.* 2004). In our study, although the external data set came from the two inner canyon branches for which no previous data were available, it did not suggest that one model consistently outperformed the other. However, the assessment clearly indicated that great care must be taken when considering prediction outputs, particularly if only a split-sample assessment was possible and if extrapolation outside of the originally sampled area was carried out.

Conclusions

Within Whittard Canyon, the highest abundance, species richness and diversity (1/D) were found on vertical structures. However, it is clear from our study that areas predicted to have such potential are very spatially limited. Out of the 100 h of benthic imagery collected, very few such walls were encountered, and our analysis suggests that less than 0.1% of the canyon's surface area may harbour a structure similarly colonized.

This study provides an example of how important ecological areas can be identified using remotely acquired acoustic sea-bed mapping techniques and a limited amount of biological information. Such an approach provides a cost-effective strategy to facilitate the location of rare biological communities and help ensure that appropriate monitoring can be implemented. Without the continued production of adequately assessed high-resolution biological maps to inform sampling designs, the spatial complexity of diversity patterns within large geomorphological features may be underestimated and rare diversity hotspots may remain difficult to find.

Acknowledgements

We would like to thank the captains, crew, technicians and scientific parties of the RRS *James Cook* cruises *JC* -010, -035 and -036, and the RV *Belgica* cruise 10/17b. The ship time for the RV *Belgica* was provided by BELSPO and RBINS–OD Nature. We would also like to acknowledge the following funding sources: MAREMAP (Natural Environment Research Council), HERMES (EU FP6 integrated project), HERMIONE (EU FP7 project, contract number 226354), COmplex Deep-sea Environments: Mapping habitat heterogeneity As Proxy for biodiversity (CODEMAP; ERC Starting Grant no. 258482). K.R is supported by funding from CODEMAP and a postgraduate scholarship (PGSD3-408364-2011) from the Natural Sciences and Engineering Research Council (NSERC-CRSNG) of Canada.

References

van Aken H.M. (2000) The hydrography of the mid-latitude Northeast Atlantic Ocean: II: the intermediate water masses. *Deep Sea Research Part I: Oceanographic Research Papers*, **47**, 789–824.

Araújo M.B., New M. (2007) Ensemble forecasting of species distributions. *Trends in Ecology & Evolution*, **22**, 42–47.

Araújo M.B., Pearson R.G., Thuiller W., Erhard M. (2005) Validation of species–climate impact models under climate change. *Global Change Biology*, **11**, 1504–1513.

Baccini A., Friedl M.A., Woodcock C.E., Warbington R. (2004) Forest biomass estimation over regional scales using multisource data. *Geophysical Research Letters*, **31**, L10501.

Baker K., Wareham V., Snelgrove P., Haedrich R., Fifield D., Edinger E., Gilkinson K. (2012) Distributional patterns of deep-sea coral assemblages in three submarine canyons off Newfoundland, Canada. *Marine Ecology Progress Series*, **445**, 235–249.

Blondel P., Gómez Sichi O. (2009) Textural analyses of multibeam sonar imagery from Stanton Banks. Northern Ireland continental shelf. *Applied Acoustics*, **70**, 1288–1297.

Bourillet J.-F., Reynaud J.-Y., Baltzer A., Zaragosi S. (2003) The 'Fleuve Manche': the submarine sedimentary features from the outer shelf to the deep-sea fans. *Journal of Quaternary Science*, **18**, 261–282.

Breiman L. (2001) Random forests. *Machine Learning*, **45**, 5–32.

Brown C.J., Smith S.J., Lawton P., Anderson J.T. (2011) Benthic habitat mapping: a review of progress towards improved understanding of the spatial ecology of the seafloor using acoustic techniques. *Estuarine, Coastal and Shelf Science*, **92**, 502–520.

Buhl-Mortensen L., Mortensen P.B. (2004) Symbiosis in deep-water corals. *Symbiosis*, **37**, 33–61.

Buhl-Mortensen P., Dolan M., Buhl-Mortensen L. (2009) Prediction of benthic biotopes on a Norwegian offshore bank using a combination of multivariate analysis and GIS classification. *ICES Journal of Marine Science: Journal du Conseil*, **66**, 2026–2032.

Buhl-Mortensen L., Vanreusel A., Gooday A.J., Levin L.A., Priede I.G., Buhl-Mortensen P., Gheerardyn H., King N.J., Raes M. (2010) Biological structures as a source of habitat heterogeneity and biodiversity on the deep ocean margins. *Marine Ecology*, **31**, 21–50.

Clark M.R., Tittensor D., Rogers A.D., Brewin P., Schlacher T., Rowden A., Stocks K., Consalvey M. (2006) *Seamounts, Deep-sea Corals and Fisheries: Vulnerability of Deep-sea Corals to Fishing on Seamounts beyond Areas of National Jurisdiction*. Census of Marine Life, UNEP-WCMC, Cambridge, UK: 111 pp.

Costello M., McCrea M., Freiwald A., Lundälv T., Jonsson L., Bett B., Weering T.E., Haas H., Roberts J.M., Allen D. (2005) Role of cold-water Lophelia pertusa coral reefs as fish habitat in the NE Atlantic. In: Freiwald A., Roberts J.M. (Eds), *Cold-Water Corals and Ecosystems*. Springer, Berlin Heidelberg: 771–805.

Crawley M. (2007). *The R Book*. John Wiley & Sons Ltd, Chichester, UK. 950 pp.

Currie D.R., Sorokin S.J. (2014) Megabenthic biodiversity in two contrasting submarine canyons on Australia's southern continental margin. *Marine Biology Research*, **10**, 97–110.

Cutler D.R., Edwards T.C., Beard K.H., Cutler A., Hess K.T., Gibson J., Lawler J.J. (2007) Random forests for classification in ecology. *Ecology*, **88**, 2783–2792.

Davies A.J., Guinotte J.M. (2011) Global habitat suitability for framework-forming cold-water corals. *PLoS ONE*, **6**, e18483.

Davies J.S., Howell K.L., Stewart H.A., Guinan J., Golding N. (2014) Defining biological assemblages (biotopes) of conservation interest in the submarine canyons of the South West Approaches (offshore United Kingdom) for use in marine habitat mapping. *Deep Sea Research Part II: Topical Studies in Oceanography*, **104**, 208–229.

De Leo F.C., Smith C.R., Rowden A.A., Bowden D.A., Clark M.R. (2010) Submarine canyons: hotspots of benthic biomass and productivity in the deep sea. *Proceedings of the Royal Society of London. Series B, Biological Sciences*, **277**, 2783–2792.

De Leo F.C., Vetter E.W., Smith C.R., Rowden A.A., McGranaghan M. (2014) Spatial scale-dependent habitat heterogeneity influences submarine canyon macrofaunal abundance and diversity off the Main and Northwest Hawaiian Islands. *Deep Sea Research Part II: Topical Studies in Oceanography*, **104**, 267–290.

De Mol L., Van Rooij D., Pirlet H., Greinert J., Frank N., Quemmerais F., Henriet J.-P. (2011) Cold-water coral habitats in the Penmarc'h and Guilvinec Canyons (Bay of Biscay): deep-water versus shallow-water settings. *Marine Geology*, **282**, 40–52.

Dolan M.F.J., Grehan A.J., Guinan J.C., Brown C. (2008) Modelling the local distribution of cold-water corals in relation to bathymetric variables: adding spatial context to deep-sea video data. *Deep Sea Research Part I: Oceanographic Research Papers*, **55**, 1564–1579.

Duffy G.A., Lundsten L., Kuhnz L.A., Paull C.K. (2014) A comparison of megafaunal communities in five submarine canyons off Southern California, USA. *Deep Sea Research Part II: Topical Studies in Oceanography*, **104**, 259–266.

Duineveld G., Lavaleye M., Berghuis E., de Wilde P. (2001) Activity and composition of the benthic fauna in the Whittard Canyon and the adjacent continental slope (NE Atlantic). *Oceanologica Acta*, **24**, 69–83.

Dullo W.-C., Flögel S., Rüggeberg A. (2008) Cold-water coral growth in relation to the hydrography of the Celtic and Nordic European continental margin. *Marine Ecology Progress Series*, **371**, 165–176.

Duros P., Fontanier C., Metzger E., Pusceddu A., Cesbron F., de Stigter H.C., Bianchelli S., Danovaro R., Jorissen F.J. (2011) Live (stained) benthic foraminifera in the

Whittard Canyon, Celtic margin (NE Atlantic). *Deep Sea Research Part I: Oceanographic Research Papers*, **58**, 128–146.

Edinger E.N., Sherwood O.A., Piper D.J.W., Wareham V.E., Baker K.D., Gilkinson K.D., Scott D.B. (2011) Geological features supporting deep-sea coral habitat in Atlantic Canada. *Continental Shelf Research*, **31** (Suppl. 2), S69–S84.

Flach E., Lavaleye M., de Stigter H., Thomsen L. (1998) Feeding types of the benthic community and particle transport across the slope of the N.W. European continental margin (Goban Spur). *Progress in Oceanography*, **42**, 209–231.

Fosså J.H., Mortensen P.B., Furevik D.M. (2002) The deep-water coral *Lophelia pertusa*; in Norwegian waters: distribution and fishery impacts. *Hydrobiologia*, **471**, 1–12.

Freiwald A., Helge Fosså J., Grehan A., Koslow T., Roberts J.M. (2004) *Cold-water Coral Reefs: Out of Sight – No Longer out of Mind*. UNEP-WCMC Biodiversity Series. UNEP/WCMC, Cambridge, UK: 84.

Frutos I., Sorbe J.C. (2014) Bathyal suprabenthic assemblages from the southern margin of the Capbreton Canyon ("Kostarrenkala" area), SE Bay of Biscay. *Deep Sea Research Part II: Topical Studies in Oceanography*, **104**, 291–309.

Gooday A.J., Aranda da Silva A., Pawlowski J. (2011) Xenophyophores (Rhizaria, Foraminifera) from the Nazaré Canyon (Portuguese margin, NE Atlantic). *Deep Sea Research Part II: Topical Studies in Oceanography*, **58**, 2401–2419.

Gori A., Orejas C., Madurell T., Bramanti L., Martins M., Quintanilla E., Marti-Puig P., Lo Iacono C., Puig P., Requena S., Greenacre M., Gili J.M. (2013) Bathymetrical distribution and size structure of cold-water coral populations in the Cap de Creus and Lacaze-Duthiers canyons (northwestern Mediterranean). *Biogeosciences*, **10**, 2049–2060.

Guisan A., Edwards T.C. Jr, Hastie T. (2002) Generalized linear and generalized additive models in studies of species distributions: setting the scene. *Ecological Modelling*, **157**, 89–100.

Hall-Spencer J., Allain V., Fosså J.H. (2002) Trawling damage to Northeast Atlantic ancient coral reefs. *Proceedings of the Royal Society of London. Series B: Biological Sciences*, **269**, 507–511.

Harris P.T., Whiteway T. (2011) Global distribution of large submarine canyons: geomorphic differences between active and passive continental margins. *Marine Geology*, **285**, 69–86.

Hastie T., Tibshirani R., Friedman J. (2009) *The Elements of Statistical Learning: Data Mining, Inference, and Prediction*. Springer, New York, USA. 763 pp.

Henry L.-A., Davies A., Murray Roberts J. (2010) Beta diversity of cold-water coral reef communities off western Scotland. *Coral Reefs*, **29**, 427–436.

Henry L.A., Moreno Navas J., Roberts J.M. (2013) Multi-scale interactions between local hydrography, seabed topography, and community assembly on cold-water coral reefs. *Biogeosciences*, **10**, 2737–2746.

Hill M.O. (1973) Diversity and evenness: a unifying notation and its consequences. *Ecology*, **54**, 427–432.

Huvenne V., Huenerbach V., Blondel P., LeBas T. (2007) Detailed Mapping of Shallow-water Environments Using Image Texture Analysis on Sidescan Sonar and Multibeam Backscatter Imagery, *In Underwater Acoustic Measurements: Technologies & Results*. Heraklion, Crete, Greece, 8 pp.

Huvenne V.A.I., Tyler P.A., Masson D.G., Fisher E.H., Hauton C., Hühnerbach V., Le Bas T.P., Wolff G.A. (2011) A picture on the wall: innovative mapping reveals cold-water coral refuge in submarine canyon. *PLoS ONE*, **6**, e28755.

Isachenko A., Gubanova Y., Tzetlin A., Mokievsky V. (2014) High-resolution habitat mapping on mud fields: new approach to quantitative mapping of Ocean quahog. *Marine Environmental Research*, **102**, 36–42.

Jenness J. (2012a) *DEM Surface Tools v. 2.1.305*. Jenness Enterprises.

Jenness J. (2012b) *Land Facet Corridor Designer, v. 1.2.848*. Jenness Enterprises.

Johnson M.P., White M., Wilson A., Würzberg L., Schwabe E., Folch H., Allcock A.L. (2013) A vertical wall dominated by *Acesta excavata* and *Neopycnodonte zibrowii*, part of an undersampled group of deep-sea habitats. *PLoS ONE*, **8**, e79917.

Jones D.O.B., Brewer M.E. (2012) Response of megabenthic assemblages to different scales of habitat heterogeneity on the Mauritanian slope. *Deep Sea Research Part I: Oceanographic Research Papers*, **67**, 98–110.

Juniper S.K., Matabos M., Mihály S., Ajayamohan R.S., Gervais F., Bui A.O.V. (2013) A year in Barkley Canyon: a time-series observatory study of mid-slope benthos and habitat dynamics using the NEPTUNE Canada network. *Deep Sea Research Part II: Topical Studies in Oceanography*, **92**, 114–123.

Kenchington E.L., Cogswell A.T., MacIsaac K.G., Beazley L., Law B.A., Kenchington T.J. (2014) Limited depth zonation among bathyal epibenthic megafauna of the Gully submarine canyon, northwest Atlantic. *Deep Sea Research Part II: Topical Studies in Oceanography*, **104**, 67–82.

Knudby A., Brenning A., LeDrew E. (2010) New approaches to modelling fish–habitat relationships. *Ecological Modelling*, **221**, 503–511.

Koleff P., Gaston K.J., Lennon J.J. (2003) Measuring beta diversity for presence–absence data. *Journal of Animal Ecology*, **72**, 367–382.

Le Bas T.P., Hühnerbach V. (1998) *PRISM Processing of Remotely-sensed Imagery for Seafloor Mapping Handbook*. Southampton Oceanography Centre, Southampton, UK. 82 pp.

Le Bas T.P., Huvenne V.A.I. (2009) Acquisition and processing of backscatter data for habitat mapping – comparison of multibeam and sidescan systems. *Applied Acoustics*, **70**, 1248–1257.

Legendre P., Fortin M. (1989) Spatial pattern and ecological analysis. *Vegetatio*, **80**, 107–138.

Lo Iacono C., Gràcia E., Diez S., Bozzano G., Moreno X., Dañobeitia J., Alonso B. (2008) Seafloor characterization and backscatter variability of the Almería Margin (Alboran Sea, SW Mediterranean) based on high-resolution acoustic data. *Marine Geology*, **250**, 1–18.

Lutz M.J., Caldeira K., Dunbar R.B., Behrenfeld M.J. (2007) Seasonal rhythms of net primary production and particulate organic carbon flux to depth describe the efficiency of biological pump in the global ocean. *Journal of Geophysical Research: Oceans*, **112**, C10011.

Marmion M., Luoto M., Heikkinen R.K., Thuiller W. (2009a) The performance of state-of-the-art modelling techniques depends on geographical distribution of species. *Ecological Modelling*, **220**, 3512–3520.

Marmion M., Parviainen M., Luoto M., Heikkinen R.K., Thuiller W. (2009b) Evaluation of consensus methods in predictive species distribution modelling. *Diversity and Distributions*, **15**, 59–69.

Matabos M., Bui A.O.V., Mihály S., Aguzzi J., Juniper S.K., Ajayamohan R.S. (2014) High-frequency study of epibenthic megafaunal community dynamics in Barkley Canyon: a multi-disciplinary approach using the NEPTUNE Canada network. *Journal of Marine Systems*, **130**, 56–68.

McArthur M.A., Brooke B.P., Przeslawski R., Ryan D.A., Lucieer V.L., Nichol S., McCallum A.W., Mellin C., Cresswell I.D., Radke L.C. (2010) On the use of abiotic surrogates to describe marine benthic biodiversity. *Estuarine, Coastal and Shelf Science*, **88**, 21–32.

Micallef A., Le Bas T.P., Huvenne V.A.I., Blondel P., Hühnerbach V., Deidun A. (2012) A multi-method approach for benthic habitat mapping of shallow coastal areas with high-resolution multibeam data. *Continental Shelf Research*, **39–40**, 14–26.

Mienis F., de Stigter H.C., White M., Duineveld G., de Haas H., van Weering T.C.E. (2007) Hydrodynamic controls on cold-water coral growth and carbonate-mound development at the SW and SE Rockall Trough Margin, NE Atlantic Ocean. *Deep Sea Research Part I: Oceanographic Research Papers*, **54**, 1655–1674.

Monk J., Ierodiaconou D., Versace V.L., Bellgrove A., Harvey E., Rattray A., Laurenson L., Quinn G.P. (2010) Habitat suitability for marine fishes using presence-only modelling and multibeam sonar. *Marine Ecology Progress Series*, **420**, 157–174.

Morell V. (2007) Into the deep: first glimpse of Bering Sea canyons heats up fisheries battle. *Science*, **318**, 181–182.

Morris K.J., Tyler P.A., Masson D.G., Huvenne V.I.A., Rogers A.D. (2013) Distribution of cold-water corals in the Whittard Canyon, NE Atlantic Ocean. *Deep-Sea Research Part II: Topical Studies in Oceanography*, **92**, 136–144.

Mortensen P., Buhl-Mortensen L. (2005) Deep-water corals and their habitats in The Gully, a submarine canyon off Atlantic Canada. In: Freiwald A., Roberts J.M. (Eds), *Cold-Water Corals and Ecosystems*. Springer, Berlin Heidelberg: 247–277.

Mortensen P.B., Buhl-Mortensen L., Gebruk A.V., Krylova E.M. (2008) Occurrence of deep-water corals on the Mid-Atlantic Ridge based on MAR-ECO data. *Deep Sea Research Part II: Topical Studies in Oceanography*, **55**, 142–152.

Orejas C., Gori A., Lo Iacono C., Puig P., Gili J.M., Dale M.R.T. (2009) Cold-water corals in the Cap de Creus canyon, northwestern Mediterranean: spatial distribution, density and anthropogenic impact. *Marine Ecology Progress Series*, **51**, 37–51.

Palialexis A., Georgakarakos S., Karakassis I., Lika K., Valavanis V.D. (2011) Prediction of marine species distribution from presence–absence acoustic data: comparing the fitting efficiency and the predictive capacity of conventional and novel distribution models. *Hydrobiologia*, **670**, 241–266.

Paterson G.L.J., Glover A.G., Cunha M.R., Neal L., de Stigter H.C., Kiriakoulakis K., Billett D.S.M., Wolff G.A., Tiago A., Ravara A., Lamont P., Tyler P. (2011) Disturbance, productivity and diversity in deep-sea canyons: a worm's eye view. *Deep Sea Research Part II: Topical Studies in Oceanography*, **58**, 2448–2460.

Puig P., Canals M., Company J.B., Martin J., Amblas D., Lastras G., Palanques A., Calafat A.M. (2012) Ploughing the deep sea floor. *Nature*, **489**, 286–289.

R Development Core Team (2011) *R: A Language and Environment for Statistical Computing*. R Foundation for Statistical Computing, Vienna: Austria.

Randin C.F., Dirnböck T., Dullinger S., Zimmermann N.E., Zappa M., Guisan A. (2006) Are niche-based species distribution models transferable in space? *Journal of Biogeography*, **33**, 1689–1703.

Reid G.S., Hamilton D. (1990) A reconnaissance survey of the Whittard Sea Fan, Southwestern Approaches, British Isles. *Marine Geology*, **92**, 69–86.

Rengstorf A.M., Yesson C., Brown C., Grehan A.J. (2013) High-resolution habitat suitability modelling can improve conservation of vulnerable marine ecosystems in the deep sea. *Journal of Biogeography*, **40**, 1702–1714.

Roberts J.M., Henry L.A., Long D., Hartley J.P. (2008) Cold-water coral reef frameworks, megafaunal communities and evidence for coral carbonate mounds on the Hatton Bank, north east Atlantic. *Facies*, **54**, 297–316.

Ross R.E., Howell K.L. (2012) Use of predictive habitat modelling to assess the distribution and extent of the current protection of 'listed' deep-sea habitats. *Diversity and Distributions*, **19**, 433–445.

Simpson E.H. (1949) Measurement of diversity. *Nature Australia*, **163**, 688.

Stewart H.A., Davies J.S., Guinan J., Howell K.L. (2014) The Dangeard and Explorer canyons, South Western Approaches UK: geology, sedimentology and newly discovered cold-

water coral mini-mounds. *Deep Sea Research Part II: Topical Studies in Oceanography*, **104**, 230–244.

Tittensor D.P., Baco A.R., Brewin P.E., Clark M.R., Consalvey M., Hall-Spencer J., Rowden A.A., Schlacher T., Stocks K.I., Rogers A.D. (2009) Predicting global habitat suitability for stony corals on seamounts. *Journal of Biogeography*, **36**, 1111–1128.

Toucanne S., Zaragosi S., Bourillet J.F., Naughton F., Cremer M., Eynaud F., Dennielou B. (2008) Activity of the turbidite levees of the Celtic-Armorican margin (Bay of Biscay) during the last 30,000 years: imprints of the last European deglaciation and Heinrich events. *Marine Geology*, **247**, 84–103.

Tyler P., Amaro T., Arzola R., Cunha M.R., de Stigter H., Gooday A., Huvenne V., Ingels J., Kiriakoulakis K., Lastras G., Masson D., Oliveira A., Pattenden A., Vanreusel A., Van Weering T., Vitorino J., Witte U., Wolff G. (2009) Europe's grand canyon: Nazaré submarine canyon. *Oceanography and marine biology: an annual review*, **22**, 46–57.

Van Rooij D., De Mol L., Le Guilloux E., Wisshak M., Huvenne V.A.I., Moeremans R., Henriet J.P. (2010a) Environmental setting of deep-water oysters in the Bay of Biscay. *Deep Sea Research Part I: Oceanographic Research Papers*, **57**, 1561–1572.

Van Rooij D., Iglesias J., Hernández-Molina F.J., Ercilla G., Gomez-Ballesteros M., Casas D., Llave E., De Hauwere A., Garcia-Gil S., Acosta J., Henriet J.P. (2010b) The Le Danois Contourite Depositional System: interactions between the Mediterranean Outflow Water and the upper Cantabrian slope (North Iberian margin). *Marine Geology*, **274**, 1–20.

Vetter E.W., Dayton P.K. (1998) Macrofaunal communities within and adjacent to a detritus-rich submarine canyon system. *Deep Sea Research Part II: Topical Studies in Oceanography*, **45**, 25–54.

Vetter E.W., Dayton P.K. (1999) Organic enrichment by macrophyte detritus, and abundance patterns of megafaunal populations in submarine canyons. *Marine Ecology Progress Series*, **186**, 137–148.

Vetter E.W., Smith C.R., De Leo F.C. (2010) Hawaiian hotspots: enhanced megafaunal abundance and diversity in submarine canyons on the oceanic islands of Hawaii. *Marine Ecology*, **31**, 183–199.

White M., Mohn C., Stigter H., Mottram G. (2005) Deep-water coral development as a function of hydrodynamics and surface productivity around the submarine banks of the Rockall Trough, NE Atlantic. In: Freiwald A., Roberts J.M. (Eds), *Cold-Water Corals and Ecosystems*. Springer, Berlin Heidelberg: 503–514.

Wilson M.F.J., O'Connell B., Brown C., Guinan J.C., Grehan A.J. (2007) Multiscale terrain analysis of multibeam bathymetry data for habitat mapping on the continental slope. *Marine Geodesy*, **30**, 3–35.

Wood S.N., Augustin N.H. (2002) GAMs with integrated model selection using penalized regression splines and applications to environmental modelling. *Ecological Modelling*, **157**, 157–177.

Supporting Information

Additional Supporting Information may be found in the online version of this article:

Figure S1. Moran's I at various lags based on all continuous 50 m sections for (A) species richness and (B) cold-water coral presence.

Figure S2. Between dive scatterplot showing components of Beta diversity:*a*' (percentage of species occurring in both samples), *b*' (percentage of species occurring in neighbouring, but not focal sample) and *c*' (percentage of species occurring in focal, but not neighbouring samples) as described by Koleff et al. (2003).

Figure S3. Relative abundance of the most common morphospecies (in grey filter/suspension feeders) whose cumulative sum represents at least 90% of the individual observed for each dive.

Figure S4. Relative abundance of the substratum type encountered in each of the canyon branches.

Figure S5. Relative abundance of the most common morphospecies (in grey filter/suspension feeders) whose cumulative sum represents at least 90% of the individual observed for each substratum type.

Figure S6. Relative abundance of the most commonly observed taxa for each 100 m depth bands: (A) across all depths for a given taxa and (B) across all taxa for a given depth band.